

respectively. Of course this back reflection is unwanted as it causes Fabry-Perot oscillations by reflecting back and forth between the input and output grating couplers.

The heights of both teeth and slot regions are chosen so that they support first-order mode. Mode chart for slab waveguide is shown in Fig. 1(b). To support two TE-like modes in the grating region, we should have $h_1, h_2 \geq 250$ nm. We choose $h_1 = 500$ nm and $h_2 = 400$ nm, respectively. The corresponding effective indices for the first-order mode in the two slabs is $n_{\text{eff}1} = 2.606$ and $n_{\text{eff}2} = 2.248$, respectively. Using (2) with an initial value of $\text{ff} = 0.5$, we get the effective index of the grating region as $n_{\text{eff}} = 2.413$.

We can choose different combinations for Λ and θ_c to achieve coupling to the first-order mode. As an initial value, we take $\theta_0 = 15^\circ$ which is the angle in air. For a SiO_2 cladding with effective index 1.444, the angle in the cladding will be $\theta_c = 10.32^\circ$. This value corresponds to a grating period of $\Lambda = 720$ nm.

2D-FDTD simulation is performed to prove the concept and optimize the coupler parameters as it takes much less computational memory and simulation time. A linear sweeping has been performed for different parameters to choose the best coupling efficiency. With all parameters chosen to get the best coupling efficiency at 1550 nm, the coupling efficiency of the input GC is 53.4% (-2.725 dB) with back-reflection less than 0.29% (-25.4 dB), Fig. 2. In this case, the coupling efficiency to TE_0 , TM_0 , and TM_1 has a maximum value of 0.4%. The taper length required to connect a $12 \mu\text{m}$ grating to a strip waveguide of 600 nm width is estimated to be hundreds micrometers [3], [4], which increases the footprint significantly.

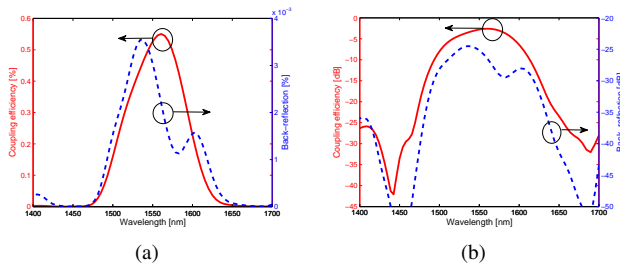


Fig. 2: Input GC coupling efficiency and back-reflection with $1 \mu\text{m}$ air-spacing between clad and fiber.

III. FOCUSING GRATING COUPLER

To keep the footprint of the grating coupler small, some curvature is introduced to the grating lines. According to the idea demonstrated in [3], a linear grating coupler can be transformed into a compact shape using focusing gratings. This can be done by curving the grating lines to take the form of confocal ellipses with the output waveguide at the focus. The grating lines follow the relation:

$$q\lambda_0 = zn_c \cos(\theta_c) - n_{\text{eff}}\sqrt{y^2 + z^2}, \quad (4)$$

where q is the grating line number, z is the direction of propagation and the grating lies in the y - z plane. Figure 3(a) shows the mode chart for a strip waveguide of height 400 nm at 1550 nm. Parameters obtained from the linear grating section is used for the focusing grating. At 600 nm, the strip waveguide supports 3 HE modes. The effective index of HE_{21} is 2.104, which matches the effective index in the grating region to reduce back-reflections. An input taper angle of 60° , shown in Fig. 3(a), and a length of $3 \mu\text{m}$ have been chosen by sweeping to get the best coupling efficiency to the single-mode fiber. The number of grating periods are found to be 19 periods with period length of 720 nm at the center of the grating, chosen from the linear grating section. A coupling efficiency of 31.7% with 1 dB bandwidth of 120 nm is obtained.

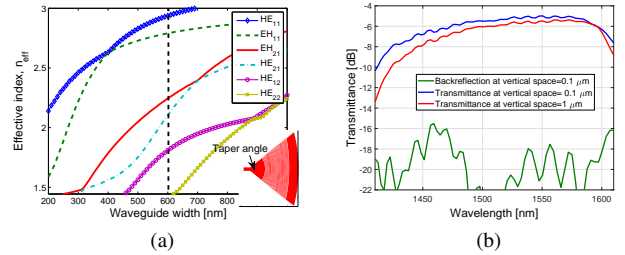


Fig. 3: (a) Mode chart of a strip waveguide at a Si height of 400 nm and a wavelength of 1550 nm. (b) Transmittance from the first-order mode in the waveguide to the fiber.

For the focusing GC, we use a single mode-fiber with core and cladding diameters of $9 \mu\text{m}$ and $125 \mu\text{m}$, respectively. The output light from the fiber is simulated as a Gaussian source. The focusing layout dimensions are $17 \mu\text{m}$ length (grating, input and output tapers) and $20 \mu\text{m}$ width, which makes it very compact.

Figure 3(b) shows the transmittance to the fiber with two values of the vertical spacing between the cladding and the fiber. As the spacing reduces to 100 nm, the transmittance is improved by 0.5 dB.

REFERENCES

- [1] P. P. Absil, P. Verheyen, P. D. Heyn, M. Pantouvaki, G. Lepage, J. D. Coster, and J. V. Campenhout, "Silicon photonics integrated circuits: a manufacturing platform for high density, low power optical I/O's," *Opt. Express*, vol. 23, no. 7, pp. 9369–9378, 2015.
- [2] M. L. Dakss, L. Kuhn, P. F. Heidrich, and B. A. Scott, "Grating coupler for efficient excitation of optical guided waves in thin films," *Appl. Phys. Lett.*, vol. 16, no. 12, pp. 523–525, 1970.
- [3] Q. Zhong, V. Veerasubramanian, Y. Wang, W. Shi, D. Patel, S. Ghosh, A. Samani, L. Chrostowski, R. Bojko, and D. V. Plant, "Focusing-curved subwavelength grating couplers for ultra-broadband silicon photonics optical interfaces," *Opt. Express*, vol. 22, no. 15, pp. 18 224–18 231, 2014.
- [4] Y. Wang, X. Wang, J. Flueckiger, H. Yun, W. Shi, R. Bojko, N. A. F. Jaeger, and L. Chrostowski, "Focusing sub-wavelength grating couplers with low back reflections for rapid prototyping of silicon photonic circuits," *Opt. Express*, vol. 22, no. 17, pp. 20 652–20 662, 2014.
- [5] C. J. Oton, "Long-working-distance grating coupler for integrated optical devices," *IEEE Photonics J*, vol. 8, no. 1, pp. 1–8, 2016.
- [6] M. Asaduzzaman, M. Bakaul, S. Skafidas, and M. R. H. Khondokar, "Compact silicon photonic grating coupler with dual-taper partial overlay-spot-size converter," *IEEE Photonics J*, vol. 9, no. 2, pp. 1–7, 2017.